

APPENDICES

APPENDIX 8A	MARINE BASELINE DESCRIPTION (NO CHANGE)
APPENDIX 8B	EFFLUENT DISPERSION MODELLING (CHANGE)
APPENDIX 8C	UNDERWATER NOISE MODELLING (CHANGE)
APPENDIX 8D	SHIP-GENERATED WAVE AND AIRCRAFT NOISE ANALYSES (NO CHANGE)

APPENDIX 8B
EFFLUENT DISPERSION MODELLING

- APPENDIX 8B-1 BALLAST WATER DISCHARGE AT STEENSBY INLET (NO CHANGE)**
- APPENDIX 8B-2 SEWAGE EFFLUENT MODELLING AT STEENSBY INLET (NO CHANGE)**
- APPENDIX 8B-3 BALLAST WATER DISPERSION AT MILNE INLET (NEW)**
- APPENDIX 8B-4 RISK ASSESSMENTS – BALLAST WATER AND HULL BIOFOULING (NEW)**

APPENDIX 8B-3

BALLAST WATER DISPERSION AT MILNE INLET

Ballast Water Discharge in Milne Inlet, Baffin Island



Isaac Fine and Alexander Rabinovich

Report Submitted

To

**Baffinland Iron Mines
Toronto, Ontario**

May 6, 2013

Executive Summary

An empirical and analytical study was undertaken of the probable fate of ballast water discharged in summer (ice-free period) for vessels proposed to transit to and dock at Milne Port as part of the Early Revenue Phase (ERP).

Results indicate that ballast water discharged from the port and starboard sides of vessels will merge within minutes into a single gravity current which will flow downslope at speeds of 0.06 to 0.24 ms^{-1} (~0.1 to 0.5 knots). It will take the head of the gravity current of about 1.5-4 hrs to travel the 900 m to the base of the slope. Tidal currents are weak in Milne Inlet, even during times of maximum tidal flow, and thus will have little time to deflect gravity currents from their downslope course. In all instances, offshore pooling of the ballast water is therefore likely to occur directly offshore, less than one kilometer from the vessel.

Over the summer discharge period, the gravity currents will diffuse laterally and vertically due to the effects of background turbulence and currents associated with tidal, wind-driven and estuarine circulation. Our findings indicate that the horizontal tidal excursion has a range from 140 m to 330 m. It is probable that the initial plume will occupy the full southern narrow part of Milne Inlet (Assumption Harbour). Vertical mixing during the summer operational season and winter ice-covered conditions will extend the thickness of the initial plume up to 20-50 m. The lateral and vertical expansion of the plume leads to a decrease in the concentration of the ballast water in the plume, which at the end of the year will be as small as 10^{-3} (~0.1%). **The final (year-round) change in water properties will contribute only a small fraction (about 0.1%) of typical natural changes of water properties occurring in the inlet on annual basis.**

Table of Contents

Executive Summary.....	2
1. Introduction.....	4
2. Basic scenarios.....	4
3. General conditions.....	5
4. Observations.....	6
5. Initial parameters.....	9
6. Short-term evolution of the discharged ballast water.....	10
6.1. Downslope gravity current.....	10
6.2. Seaward extent of the ballast water gravity current.....	13
6.3. Offshore confinement of the ballast water by rotational forces.....	14
7. Long-term changes in the initial plume due to background circulation in the bay.....	15
7.1. Tides and tidal currents.....	15
7.2. Wind-induced currents and estuarine circulation.....	22
7.3. Vertical mixing scale.....	23
8. Estimation of the water property change in Milne Inlet related to summer operations	24
9. Conclusions.....	26
10. References.....	28

1. Introduction

The main purpose of this report is to consider the fate of ballast water discharged in summer (ice-free period) from vessels docked in Milne Inlet. We assume that the ballast water, taken aboard ship from the salty water in the Mid-Atlantic or Labrador Sea, has a much greater density than that in Milne Inlet. Parameters of Milne Inlet water were determined based on three series of CTD observations collected in the summers 2008 and 2010.

The updated (2013) shipping and discharge scenarios are significantly different from the original 2010 scenarios analysed. The changes in the scenario are expected to have a marked effect on the final dilution values. The main purpose of the present report is to consider the fate of ballast water discharged in summer for this new shipping scenario. We also supplemented and improved the previous tidal analysis and added an estimation of the ballast water plume extension associated with vertical mixing and horizontal advection by estuarine and wind-induced circulation.

We were requested to undertake a preliminary estimation of the dispersal of ballast water discharged at the proposed port site in Milne Inlet from iron ore bulk carriers. Here, we present a preliminary analysis of the probable dispersion pathways and concentrations of the ballast water spread throughout the inlet under the influence of gravity currents and typical oceanographic conditions that likely occur in the inlet.

2. Basic scenarios

The basic scenarios provided are:

- The ballast water originates from the Mid-Atlantic or Labrador Sea.
- The ballast water discharge will be confined to a ninety-day period from mid-July to mid-October each year.

- There will be a discharge averaging 1,000 tonnes per hour (average of 12,500 tonnes; range = 9,600 – 21,600) over 12 of the 24 hours each vessel spends dockside. A total discharge of approximately 662,000 tonnes of ballast water each shipping season.
- The 12 hours of ballast water discharge dockside will occur 53 times between July 15 and October 15 each year.

3. General conditions

Milne Inlet is located on the northwestern coast of Baffin Island. It extends in a southerly direction from Navy Board Inlet at the confluence with Eclipse Sound. Bylot Island shelters Milne Inlet from Baffin Bay and Lancaster Sound. Eclipse Sound (south of Bylot Island) connects Milne Inlet with Baffin Bay. Navy Board Inlet (west of Bylot Island) connects Milne Inlet with Lancaster Sound (Figure 1).

The meteorological conditions in this region are quite severe and are strongly influenced by the North American and Greenland land masses and by the Arctic atmospheric system. The mean winter temperature is -35 °C, while the mean summer temperature is +4.5 °C. Winds are usually about 5 m/s; weather systems normally move from the west and southwest [Tang *et al.*, 2004; McLaughlin *et al.*, 2006]. The main factor influencing navigation in the region adjacent to Milne Inlet is sea ice; most of the year the northern part of Baffin Bay, including Milne Inlet, is covered by highly concentrated ice. The circulation in Baffin Bay is determined by the northward West Greenland Current moving along the Greenland coast, and the southward Baffin Current that moves along the shelf edge of western Baffin Bay [Fissel *et al.*, 1982; Tang *et al.*, 2004]. The Baffin Current is the primary reason there is always more ice cover along the Baffin Island (southwestern) coast of the bay than along the Greenland (northeastern) coast. Normally, minimum ice cover is observed in September [Tang *et al.*, 2004]. The water in Baffin Bay has two sources – the Arctic Ocean and Atlantic Ocean; a cold, low-salinity upper layer is present throughout the Bay, including Milne Inlet. Currents are the primary driver in the distribution and movement of sea ice, and water mass transport. However, particularly in Milne Inlet, there is no noticeable circulation except for tidal currents. Tides in this region are predominantly

semidiurnal; typical amplitudes of the tidal currents in the northwestern part of Baffin Bay are 10-20 cm s^{-1} [Fissel, 1982; Church *et al.*, 2007].

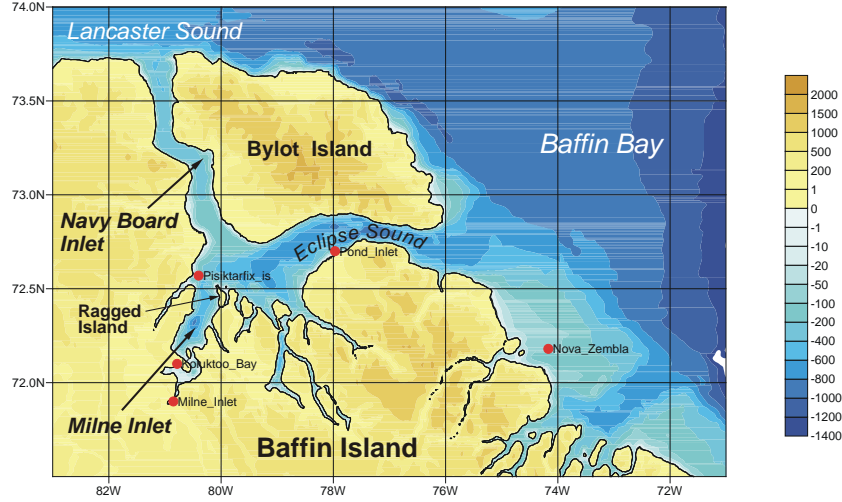


Figure 1. Location of Milne Inlet on the northwestern coast of Baffin Island. Red circles denote positions of tide gauge measurements of sea level oscillations.

4. Observations

To determine the oceanic parameters for Milne Inlet waters, we used three sets of observations (Figures 2 and 3):

- (1) CTD measurements at MCTD stations in June 2008 (MCTD-1 – MCTD-6);
- (2) CTD measurements at KCTD stations in September 2008 (KCTD-1 – KCTD-5);
- (3) Zooplankton observations with CTD measurements (Z1-Z10) and benthic samples with CTD data only at Station B-10 in August 2010.

Based on these data, we estimated sigma-*t* for the surface and a depth of 30 m, where sigma-*t* = (density – 1000) and density is measured in units of kilograms per cubic meter (kg m^{-3}). In general, the results (Tables 1 and 2) were consistent and the differences between water parameters estimated at different stations were small. We used the data from each set of

measurements to estimate *mean parameters* (the density of the receiving water, ρ_{Milne} and sigma- t) and used these parameters (presented in Table 3) for the following calculations.

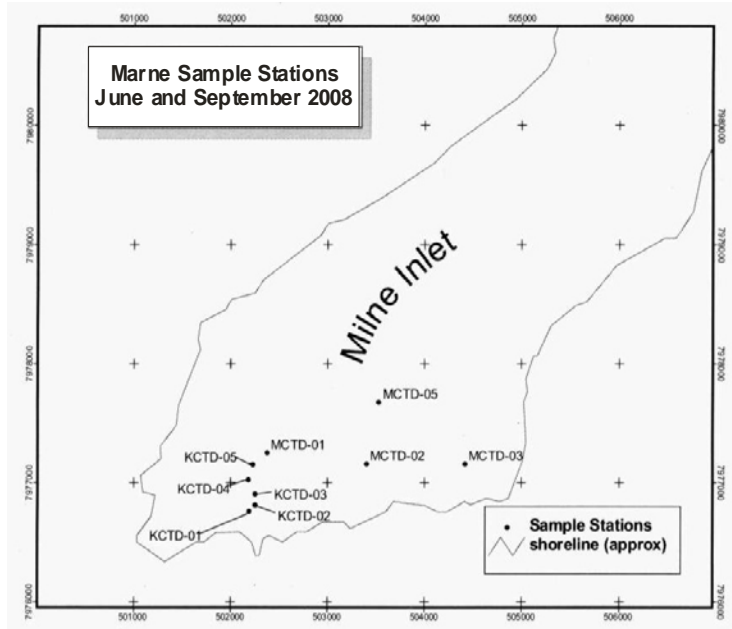


Figure 2. Marine sample stations in Milne Inlet; June and September 2008 surveys.

Table 1. Salinity, water temperature and density at Milne Inlet in June and September 2008 (based on CTD measurements; locations of the sites are shown in Figure 2)

Station	Depth					
	0 m			30 m		
	Temperature (°C)	Salinity (psu)	Sigma- t (kg m $^{-3}$)	Temperature (°C)	Salinity (psu)	Sigma- t (kg m $^{-3}$)
June 2008						
MCTD 1	2.5	2.0	1.6	-1.0	32.5	26.1
MCTD-2	1.1	2.0	1.5	-1.0	32.5	26.1
MCTD-3	1.3	3.0	2.3	-1.0	32.5	26.1
MCTD-4	0.8	2.0	1.5	-1.1	32.5	26.1
MCTD-6	0.0	1.0	0.7	-1.1	32.6	26.2
Mean	1.1	2.0	1.5	-1.0	32.5	26.1
September 2008						
KCTD-1	2.5	27.0	21.5	0.5	32.4	26.0
KCTD-2	1.6	28.0	22.4	0.6	32.4	26.0
KCTD-3	1.8	27.2	21.7	-	-	-
KCTD-4	2.6	27.9	22.3	-	-	-
KCTD-5	2.2	26.6	21.2	-	-	-
Mean	2.1	27.3	21.7	0.5	32.4	26.0

Table 2. Salinity, water temperature and density at Milne Inlet in August 2010 (based on CTD measurements; locations of the sites are shown in Figure 3)

Station	Depth					
	0 m			30 m		
	Temperature (°C)	Salinity (psu)	Sigma- <i>t</i> (kg m ⁻³)	Temperature (°C)	Salinity (psu)	Sigma- <i>t</i> (kg m ⁻³)
August 24, 2010						
Series 3	7.5	21.0	16.4	-0.3	31.5	25.3
Series 4	7.5	23.0	17.9	-0.3	31.5	25.3
Series 5	8.0	21.5	16.7	-0.3	31.5	25.3
Series 6	7.5	22.5	17.5	-0.2	31.5	25.2
Series 7	7.3	23.2	18.1	-0.5	31.7	25.5
Series 8	7.3	23.2	18.1	-0.5	31.3	25.1
Series 9	8.0	17.5	13.6	-0.3	31.4	25.2
Series 10	7.5	21.5	16.8	-0.4	31.5	25.3
Series 11	7.8	18.0	14.0	-0.4	31.5	25.3
August 22-28, 2010						
B10	6.5	25.0	19.6	-0.3	31.5	25.3
Mean	7.5	21.6	16.9	-0.3	31.5	25.3

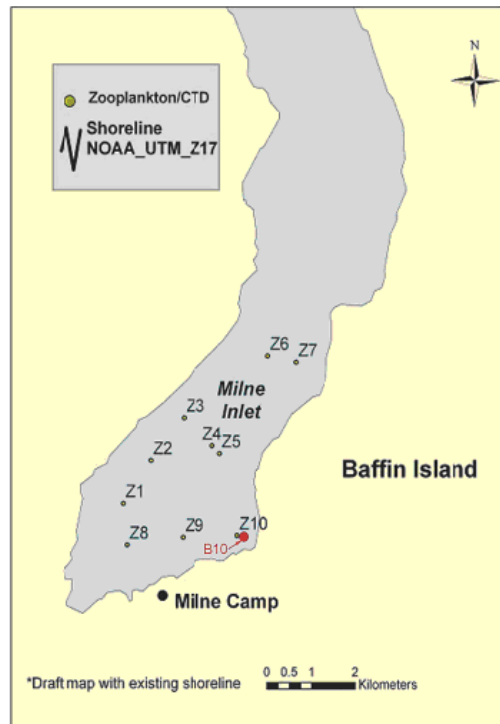


Figure 3. Zooplankton and benthic stations with CTD measurements in Milne Inlet; August 2010 survey.

Table 3. Observed temperature, salinity, and density at near-surface and 30 m depth in Milne Inlet. Density values are used for estimating the fate of ballast water discharged during summer months.

Observational period	Temperature (°C)		Salinity (psu)		Sigma-t (kg m ⁻³)		Density, ρ_{Milne} (kg m ⁻³)	
	Surface	30 m	Surface	30 m	Surface	30 m	Surface	30 m
June 2008	1.1	-1.0	2.0	32.5	1.5	26.1	1001.5	1026.1
September 2008	2.1	0.5	27.3	32.4	21.7	26.0	1021.7	1026.1
August 2010	7.5	-0.3	21.6	31.5	16.9	25.3	1016.9	1025.3

Melting of sea ice in summer generates formation of a thin, strongly stratified, upper layer with highly desalinated water. As seen in Tables 1-3, the salinity and temperature in this layer are highly variable in space and time. The typical thickness of this layer is 0.5 to 1.5 m. Tides and associated tidal currents are the main factor contributing to the vertical mixing and weakening of this stratified layer.

5. Initial parameters

The ballast water is to be discharged in summer over a period of 12 hours from a vessel docked in Milne Inlet. We assume simultaneous point-source discharge from the port and starboard sides of the vessel near the water line in water depths of 25 to 30 m. The Labrador Sea ballast water is assumed to have an *in situ* density (sigma-t) of 26.76 in summer. The density of the ballast water is significantly greater than that of the receiving water in Milne Inlet.

The following parameters have been used in the analysis:

Summer ballast water volume discharge, Q: Volume discharge is 1000 m³ (1000 tonnes = 1000 m³) over a one-hour period, whereby $Q = 0.28 \text{ m}^3 \text{s}^{-1}$. This is the combined discharge rate for both the port and starboard discharge points.

Summer ballast water density (sigma-*t*): 26.76 ($\rho_{ballast} = 1026.76 \text{ kg m}^{-3}$) based on a year-round salinity of ~ 34.0 psu and summer water temperature of around 6°C .

Summer receiving water density (sigma-*t*): We consider three cases (see Table 3): (a) sigma-*t* from 1.5 near the surface to 26.1 at 30 m depth ($\rho_{Milne} = 1001.5$ to 1026.1); (b) sigma-*t* from 21.7 near the surface to 26.0 at 30 m depth ($\rho_{Milne} = 1021.7$ to 1026.0); and (c) sigma-*t* from 16.9 near the surface to 25.3 at 30 m depth ($\rho_{Milne} = 1016.9$ to 1025.3).

Discharge is assumed to occur just above the water surface (~ 0 m elevation) in water depths of 25 to 30 m. If there is an alongshore tidal and/or wind-driven current at the time of discharge, the discharge will behave slightly more like a line-source than a point-source.

Bottom slopes for Milne Inlet are quite steep: for the first ~ 200 m seaward from the ship at the dock, bottom slopes are variable but generally range from about $9\text{--}11^\circ$ and span water depths between 30 and 50 m. For distances of roughly 200 m to 900 m offshore from the ship, bottom slopes decrease to $\sim 5^\circ$ (water depths of 90 and 100 m), while for distances of 900 to 2000 m offshore, slopes are $\sim 1.75^\circ$ (water depths between 100 and 200 m). Beyond this, bottom slopes are locally variable but generally less about 1.0 to 1.25° at water depths greater than 200 m.

Tidal currents are principally semidiurnal; they are evaluated for Milne Inlet based on results of tidal observations in this region and results of a simple analytical estimation.

6. Short term evolution of the discharged ballast water

6.1. Downslope gravity current

The above parameters have been used to provide an empirical estimate of the fate of the seafloor gravity (density) current generated during ballast water discharge from the sides of the vessel. The advance of the gravity current traveling down a slope of angle θ measured relative to the horizontal has been investigated in laboratory experiments [Bitter and Linden, 1980]. According

to this study, the head of the gravity current advances at a speed U_f which satisfies the relationship

$$\frac{U_f}{(g'Q/W)^{1/3}} = 1.5 \pm 0.2 \quad (1)$$

for slope angles $5^\circ \leq \theta \leq 90^\circ$, where W is the width of the discharge flow parallel to the alongshore direction at the point of entry into the inlet, and

$$g' = g \frac{\Delta\rho}{\rho_{Milne}} \quad (2)$$

is the “reduced gravity” based on a water density, ρ_{Milne} , in Milne Inlet. Here, $g = 9.81 \text{ ms}^{-2}$ is the acceleration of gravity, and

$$\Delta\rho = \rho_{ballast} - \rho_{Milne} \quad (3)$$

is the difference in density between the ballast water and the ambient receiving water in Milne Inlet at the point of discharge.

Summer downslope gravity current

The water density in the upper 30 m of Milne Inlet in summer is assumed to have a density $\rho_{Milne} = 1001.5 - 1021.7 \text{ kg m}^{-3}$ ($\sigma_t = 1.5 - 21.7$) near the surface and $\rho_{Milne} = 1025.3 - 1026.1 \text{ kg m}^{-3}$ ($\sigma_t = 25.3 - 26.1$) at 30 m, while the Labrador Sea ballast water has a density $\rho_{ballast} = 1027.17 \text{ kg m}^{-3}$.

Using the above density values, we estimated the difference in density, $\Delta\rho = \rho_{ballast} - \rho_{Milne}$, and estimated the reduced gravity, g' . Then, using this set of parameters and equation (1), we estimated that the one-meter wide ($W = 1 \text{ m}$) discharge ports on the starboard and port sides of the vessel will give rise to downslope gravity currents with speeds of advance

$$U_f = 1.5 (g' Q/W)^{1/3} . \quad (4)$$

Results of the analysis are presented in Table 4. Set 1 is based on CTD measurements for June 2008, Set 2 for September 2008, and Set 3 for August 2010 (see Table 3).

Table 4. Summer downslope velocity, U_f , the head of a gravity current for a ballast volume discharge $Q = 0.28 \text{ m}^3 \text{s}^{-1}$ and the ballast water density $\rho_{ballast} = 1026.76 \text{ kgm}^{-3}$.

Set, depth	Milne Inlet water density, ρ_{Milne} (kgm^{-3})	Density difference, $\Delta\rho$ (kgm^{-3})	Reduced gravity, g' (ms^{-2})	Downslope gravity current, U_f (ms^{-1})
Set 1, surface	1001.5	25.26	0.2474	0.42
30 m	1026.1	0.66	0.0063	0.12
Set 2, surface	1021.7	5.06	0.0485	0.24
30 m	1026.1	0.66	0.0063	0.12
Set 3, surface	1016.9	9.86	0.0951	0.30
30 m	1025.3	1.46	0.0140	0.16

According to these results, it will take the gravity currents 2 to 6 minutes to progress downslope from one side of the ship to the other. Because the gravity current formed on the upslope side of the ship will rapidly merge with the gravity current formed on the downslope side of the ship, we are justified in treating the combined discharge as one value

$$Q = 0.28 \text{ m}^3 \text{s}^{-1} \quad (5)$$

as if the discharge for the port and starboard sides of the vessel contribute simultaneously to the generation of a single gravity current on the downslope side of the vessel. Table 5 provides estimates of the gravity current speed, U_f , for Set 2 (which can be considered as the “most typical”) of the summer water density in Milne Inlet ($\rho_{surface} = 1021.7$ at the surface and $\rho_{bottom} = 1026.1$ at 30 m depth) for a range of ballast discharge widths, W .

Table 5. Downslope velocity, U_f , of the head of a gravity current for a ballast volume discharge $Q = 0.28 \text{ m}^3 \text{s}^{-1}$ for the ballast water density $\rho_{\text{ballast}} = 1026.76 \text{ kgm}^{-3}$, receiving water densities (ρ_{Milne}), and various values of the alongshore discharge width, W .

	ρ_{ballast} (kg/m ³)	ρ_{Milne} (kg/m ³)	W (m)	U_f (m/s)
ρ_{surface}	1026.76	1021.7	1	0.24
	1026.76	1021.7	2	0.19
	1026.76	1021.7	5	0.14
	1026.76	1021.7	10	0.11
ρ_{bottom}	1026.76	1026.1	1	0.12
	1026.76	1026.1	2	0.10
	1026.76	1026.1	5	0.07
	1026.76	1026.1	10	0.06

6.2. Seaward extent of the ballast water gravity current

The empirical calculations in the previous sections reveal that for a discharge “footprint” of 1 to 10 m and water densities in the upper 30 m of Milne Inlet close to those observed near the inlet surface, the head of the gravity current will advance down the sloping bottom of the inlet at velocities of $U_f \sim 0.06$ to 0.24 ms^{-1} . Results for this model are valid until the gravity current reaches an offshore distance of roughly 900 m whereupon the current will begin to slow considerably due to frictional effects as the bottom slope diminishes to near zero in the offshore direction. With maximum downslope speeds in excess of 0.06 ms^{-1} , it will typically take ballast water about four hours to advance 900 m offshore to the flatter regions of the bottom where average slopes diminish to less than 2° . For a downslope speed of 0.10 ms^{-1} , the time to advance 900 m offshore is about 1.5 hrs. On the basis of these results, we expect the relatively warm, salty ballast water to begin to “pool” over the slope while advancing much more slowly to deeper water beyond 900 m.

6.3. Offshore confinement of the ballast water by rotational forces

In addition to the downslope loss of speed associated with the diminishing slopes and increasing depth, the offshore extent of the gravity current will also be affected by Coriolis (rotational) effects as it moves downslope. Due to the Earth's rotational effects, the time-averaged downslope flow will assume a radius of curvature, r , given by

$$r = \frac{U}{f}, \quad (6)$$

where U is the downslope speed and f is the Coriolis parameter

$$f = 2\Omega \sin(\varphi), \quad (7)$$

where φ is the geographical latitude and $\Omega = 0.72921 \times 10^{-4} \text{ s}^{-1}$ is the Earth's rate of rotation. For the proposed dock site in Milne Inlet (latitude = 71.89° N) we obtain $f = 1.3861 \times 10^{-4} \text{ s}^{-1}$ (the inertial period $T_f = 2\pi/f = 12.59$ hrs). Using $U \approx 0.1\text{--}0.2 \text{ ms}^{-1}$, we obtain

$$r \approx 0.7 - 1.5 \text{ km}$$

These distances – which are close to the offshore extent $r \approx 1 \text{ km}$ of the gravity current based on the diminishing bottom slope – provide a very rough estimate of the maximum offshore extent possible for the gravity current irrespective of the bottom slope. The 12-hour discharge period is comparable to the time $T_f = 12.59$ hrs of the inertial period associated with Coriolis effects to become fully established. This, in turn, suggests that within the time that the ballast water discharge is taking place, an alongshore geostrophic bottom current can be set up, which adds a weak to moderate northward advective flow. As a consequence, the bottom currents near the vessel will consist of a slow northward drift on which are superimposed back-and-forth semidiurnal tidal motions. This northward geostrophic current will help advect the high salinity, high temperature ballast water along the slope as it diffuses and mixes over time.

We further speculate that the patch of ballast water discharged during each visit to the Milne Inlet dock site will deform into a relatively warm, high salinity clockwise-rotating “ballast-water eddy” over the sloping bottom seaward of the vessel. We anticipate that each eddy will self-advect to the north along the slope while slowly moving into deeper water. In particular, if we assume that diffusion and viscosity cause the thickness, h , of bottom-hugging ballast water eddies to increase with time and the relative vorticity, ζ (shear in the current velocity field) of

each eddy to decrease with time, the “conservation of vorticity” requirement [Gill, 1982] for an eddy

$$\frac{f + \zeta}{h} = \text{constant} \quad (8)$$

indicates that each ballast-water eddy will move to higher latitudes (increasing Coriolis parameter, f) with time. If this analysis is correct, ballast-water eddies will maintain their integrity for considerable time (days to weeks) while slowly moving northward along the outer slope centered at a distance greater than approximately 600 m seaward of the vessel. Such translation speeds for topographically trapped eddies is typically of the order of a few centimeters per second.

7. Long term changes in the initial plume due to background circulation in the bay

7.1. Tides and tidal currents

Tides and tidal currents play a major role in determining the dynamic and hydrological characteristics of the Canadian Arctic Archipelago and, in particular, in the circulation and water mass transport in the region of Milne Inlet [Fissel *et al.*, 1982; Fissel, 1982; McLaughlin *et al.*, 2006]. The waters in this area are significantly modified by tidally-driven mixing. Five temporary tide gauges were maintained by the Canadian Hydrographic Service (CHS) from 1964-1988 in the northwestern part of Baffin Bay and in the vicinity of Milne Inlet (Figure 1, Table 6). Because of the stability of oceanic tides, these data can be used for tidal prediction and for constructing tidal models [cf. Church *et al.*, 2007].

Table 6. Tide gauge sea level observations in the northwestern part of Baffin Bay.

Station name	Station ID	Latitude (°N)	Longitude (°W)	Period of observations
Milne Inlet	5791	71.90	80.85	27/7/1965-28/9/1965
Koluktoo Bay	5790	72.10	80.78	29/7/1964-28/8/1964, 27/7/1965-01/09/1965
Pisiktarfik Island	5813	72.57	80.40	09/09/1966-24/09/1966
Pond Inlet	5800	72.7	77.97	27/08/1982-05/05/1983
Nova Zembla Island	3916	72.18	74.83	28/08/1988-28/09/1988

The mean amplitudes and phases for the tidal constituents at the sites in Table 6 were calculated using the least squares method; the results for the six major tidal harmonics are presented in Table 7. These amplitudes and phases can be used to predict tides at the corresponding sites for any period of time. Subsequently, predictions were obtained for all of the above sites for the period from June 1 to September 30, 2008; i.e. for the period when CTD measurements were available for Milne Inlet. As an example, Figure 4 shows the predicted tides at the “Milne Inlet” site.

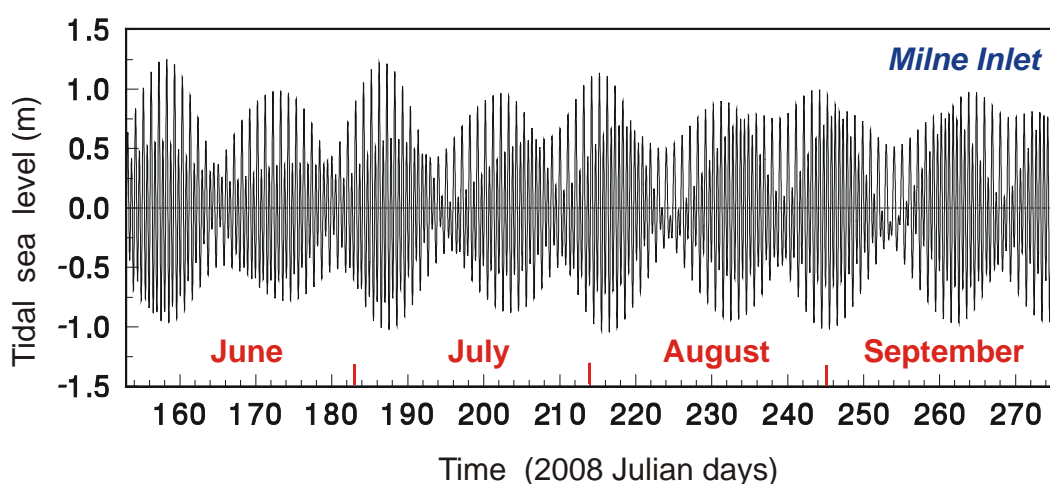


Figure 4. Predicted tidal sea level oscillations in Milne Inlet for the period June 1 – September 30, 2008.

Table 7. Calculated tidal amplitudes and phases at five sites located in the vicinity of Milne Inlet (see Figure 1 for the exact locations). The parameter F (the tidal factor; equation 9) is the ratio of diurnal to semidiurnal tidal amplitudes.

Tidal harmonic	Milne Inlet		Koluktoo Bay		Pisiktarfik Island		Pond Inlet		Nova Zembla Island	
	H (cm)	G (°)	H (cm)	G (°)	H (cm)	G (°)	H (cm)	G (°)	H (cm)	G (°)
Q_1	1.3	180.9	0.3	251.9	0.8	261.9	0.7	200.0	0.9	134.2
O_1	7.3	207.0	8.1	213.8	7.7	207.4	8.8	211.0	7.9	202.8
K_1	23.3	262.9	25.7	264.2	23.0	249.4	25.8	252.6	20.9	257.5
N_2	12.2	103.0	12.8	105.5	18.1	103.5	11.4	110.6	10.3	114.3
M_2	56.5	137.2	57.8	139.9	51.6	134.3	53.8	136.7	41.5	139.6
S_2	23.5	187.6	19.3	196.6	26.6	178.7	18.6	179.9	18.9	182.5
F	0.38		0.44		0.39		0.48		0.48	

The values in Table 7 clearly indicate that tides at this site have a dominant semidiurnal character, modulated by a pronounced fortnightly spring-neap cycle. The predicted records for other sites are almost identical, except that the amplitudes of the tides are slightly different. The main statistical parameters for the calculated tidal sea levels are presented in Table 8. At four sites located in Milne Inlet, or in the vicinity of this inlet (Milne Inlet, Kaluktoo Bay, Pisiktarfik Island and Pond Inlet), these parameters are very similar; specifically, variance values are from 2107 to 2338 cm², RMS values from 45.9 to 48.4 cm, and tidal range (minimum to maximum) from 220 to 237 cm. Only at Nova Zembla, located southeastward from the other stations (see Figure 1), are the tidal variance, RMS and tidal range considerably smaller.

The results presented in Tables 7 and 8, demonstrate that semidiurnal tides strongly prevail in this region. The tidal factor

$$F = \frac{K_1 + O_1}{M_2 + S_2} \approx 0.38 - 0.48, \quad (9)$$

indicates that tides in this region are semidiurnal or mixed semidiurnal. The dominance of semidiurnal motions should be especially true for tidal currents, because currents are related to the sea level rate of change, which normally is inversely proportional to the period and, for semidiurnal tides, twice as large as for diurnal tides (for the same sea level tidal amplitudes).

Table 8. Statistical parameters of tidal sea level variations at the Milne Inlet station based on 4-month (June-September 2008) computed tides.

Parameters	Milne Inlet	Koluktoo Bay	Pisiktarfik Island	Pond Inlet	Nova Zembla
Variance (cm ²)	2275.7	2337.9	2205.7	2106.6	1385.1
RMS (cm)	47.70	48.35	46.97	45.90	37.20
Maximum sea level (cm)	124.8	124.9	126.9	119.5	99.7
Minimum sea level (cm)	-104.4	-104.5	-110.6	-100.0	-85.2

To estimate the tidal currents, we use the relationship between the current (u) and sea level elevation (ζ) for a small semi-closed basin:

$$uS_0 = A \frac{d\zeta}{dt}, \quad (10)$$

where S_0 is the cross-section of the basin, u is the current velocity component normal to the cross-section, and A is the horizontal area from the head of the basin to the respective cross-section. Equation (1) can be transformed to

$$U_i = \frac{2\pi}{T_i} \frac{A}{S_0} H_i, \quad (11)$$

where H_i is the amplitude of the corresponding i th constituent, T_i is the respective period and U_i is the current amplitude. The results of the tidal current calculations for four cross-sections in Milne Inlet (AA', BB', CC, and DD' in Figure 5), are shown in Table 9. According to these calculations, tidal currents in Milne Inlet are weak, probably due to the relatively large depths.

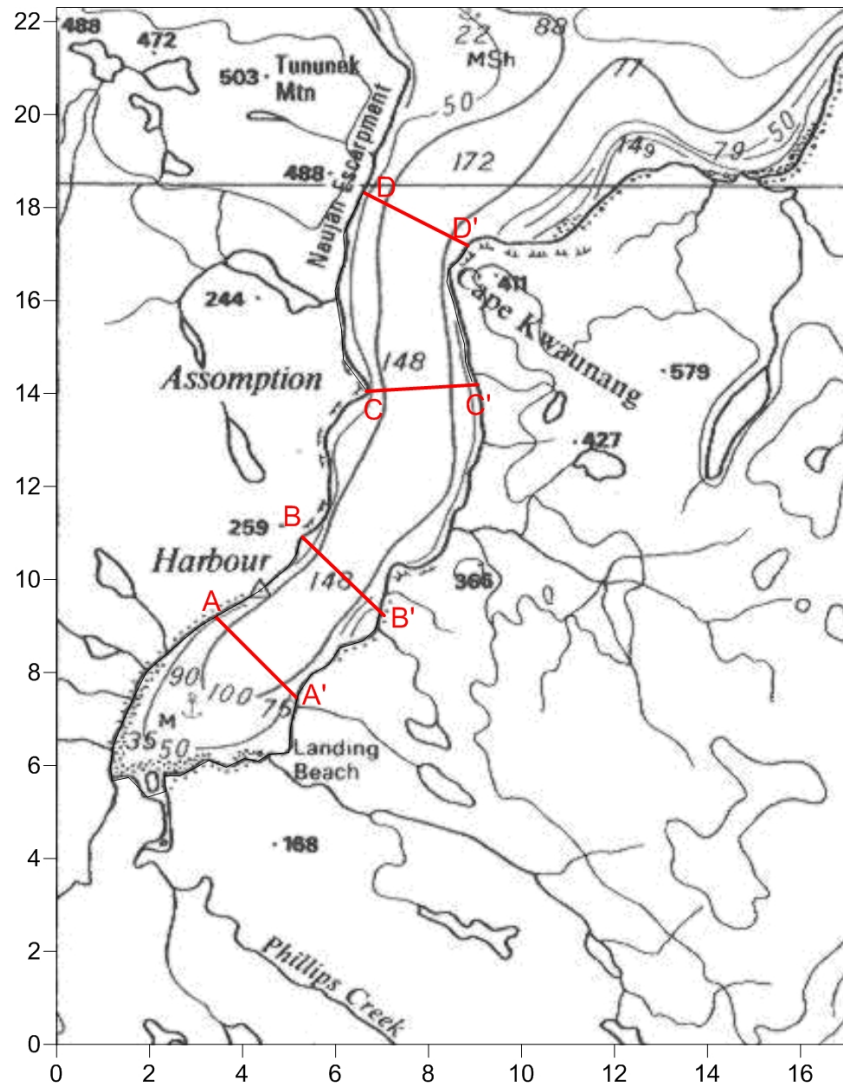


Figure 5. Cross-sections in Milne Inlet were used for calculations of the tidal currents.

Table 9. Parameters of tidal currents in Milne Inlet for three different cross-inlet sections

Cross-section	Cross-section area, S_0 (km 2)	Horizontal area toward the Inlet end, A (km 2)	Area ratio, A/S_0	M_2 current amplitude (cm/s)	Max tidal current (cm/s)
AA'	0.15	9.25	60	0.5	1.0
BB'	0.23	14.91	64	0.5	1.0
CC'	0.23	27.02	117	0.9	1.8
DD'	0.25	36.19	145	1.1	2.2

These estimates are very approximate. Irregularities in the coastline geometry and bottom topography can produce notable local amplification of the tidal currents. Our empirical estimates yield only the *barotropic* tidal currents, whereas the actual currents are *baroclinic*. Baroclinic tidal currents at *near-critical latitudes* could possibly be several times stronger than the barotropic currents we have estimated in this study [cf. *Kulikov et al.*, 2004].

The “critical latitude” is the latitude where the tidal frequency, ω_j , for j th tidal constituent is equal to the inertial frequency, $f = 2\Omega\sin(\varphi)$, where φ is the geographical latitude and $\Omega = 0.72921 \times 10^{-4}$ s $^{-1}$ is the Earth’s rate of rotation. For the proposed dock site in Milne Inlet ($\varphi = 71.89^\circ$ N) we obtain $f = 1.3861 \times 10^{-4}$ s $^{-1}$ (the inertial period $T_f = 2\pi/f = 12.59$ hrs). The major semidiurnal tidal constituents have the following periods and critical latitudes:

	T (hrs)	φ_{crit} (deg)
N_2	12.6583	70.9797;
M_2	12.4206	74.4717;
S_2	12.0000	85.7650;

As these calculations show, Milne Inlet is quite close to the critical latitudes for the N_2 and M_2 tidal harmonics. *Munk and Phillips* [1968] proposed a mechanism for resonant amplification of internal tidal currents near critical latitudes. *Kulikov et al.* [2004] examined this effect for the

Beaufort Sea shelf and found significantly amplified semidiurnal baroclinic currents. We assume that this effect may also be important for Baffin Bay, in particular, for the region near Milne Inlet. This effect could be examined using ADCP current measurements and/or by formulating a numerical model of the baroclinic tidal currents for this region.

Using the previously derived tidal parameters and our one-dimensional barotropic model for the tidal currents, we can estimate typical horizontal tidal excursions of the ballast water. Integration of equation (10) over time yields a simple linear expression relating the horizontal tidal excursion, $x(t)$, to the vertical tidal displacement, $h(t)$:

$$x(t) = \frac{A}{S_0} h(t). \quad (12)$$

According to equation (12), the horizontal tidal excursion statistics can be easily determined for each cross-section of Milne Inlet using the vertical movement for the inlet provided in Table 8. The corresponding estimates are presented in Table 10.

Table 10. Statistical parameters of the tidal excursion.

Cross-section	Variance (m ²)	RMS (m)	Maximum lateral excursion toward the inlet head (m)	Maximum lateral excursion toward the inlet mouth (m)	Total lateral excursion range (m)
AA'	819	28.6	75	62	137
BB'	932	30.5	80	67	147
CC'	3115	55.8	146	122	268
DD'	4785	69.2	181	151	332

7.2. Wind-induced currents and estuarine circulation

Estuarine circulation is related to the fresh water discharge and entrainment processes at the bottom of the upper mixing layer. The classical 2-layer circulation can be estimated in terms of a simple "box" model which includes two conservation equations. The first equation is the conservation of salinity flux through the cross-section of the inlet, which can be written in the form

$$s_u M_u + s_b M_b = 0, \quad (13)$$

where s is the salinity, M is the mass transport and indices u and b mean the upper and bottom layers. The second equation expresses the conservation of water mass at the head of the inlet (and inward from the cross-section of the inlet):

$$M_u + M_b = M_r \quad (14)$$

where M_r is the river discharge. The substitution of M_u from (14) and (13) leads to a single equation for the bottom mass flux:

$$M_b = -\frac{s_u}{s_b - s_u} M_r \quad (15)$$

The minus sign means that the bottom layer flux is directed toward the head of the inlet, counter to that in the surface layer.

In a typical, mid-latitude, well-mixed estuary, the upper- and bottom-layer salinities are nearly identical; as a consequence, the bottom mass flux exceeds the river discharge by many times. However, at high latitudes, this assumption is not always valid because of the formation of surface lenses of fresh water arising from the melting of sea ice. According to Table 3, the bottom layer estuarine flux in June was less than 7% of the river discharge. In August, however, it was likely almost two times larger than the river discharge and in September it would have exceeded 5.35 times the river discharge.

The river discharge is mainly from Phillips Creek, which flows in along the southern edge of the inlet. We assume that the creek discharge is in the range $10^1\text{-}10^2 \text{ m}^3\text{s}^{-1}$. In this case, and taking into account the cross-section area of the upper inlet is $0.15\cdot10^6 \text{ m}^2$ (Line AA', Table 9), we

estimate that the bottom inflow current to be up to 0.13 cms^{-1} in August and up to 0.35 cms^{-1} in September

Wind-induced currents will contribute additional input into the bottom layer circulation. There is no simple method to estimate bottom currents related to wind forcing. In this case, we have speculated that the wind forcing conditions (wind speed, direction and their statistics) in the Milne Inlet area are similar to those in Steensby Inlet. Although the shapes, depths, and orientation of the inlets are different, we expect that the bottom currents in Milne Inlet are of the same order of magnitude as the bottom currents in Steensby Inlet; i.e., 0.5-2 cm/s. Also, it is likely that, due to the Coriolis effect, the current at the port site will be directed toward the inlet mouth.

Table 11. The horizontal extension of the ballast water plume in Milne Inlet due to quasi-steady circulation.

Current speed (cm/s)	Plume length (km) for specified time durations		
	10 days	45 days	90 days
0.5	4.3	19	39
1	8.6	39	78
2	17.2	78	156

7.3. Vertical mixing scale

After its initial discharge, the ballast water plume will undergo vertical dispersion. This dispersion will depend on the degree of vertical turbulent mixing. In the ocean, vertical mixing is highly variable and depends on many factors, including the intensity of the currents, vertical stratification, wind forcing and many other processes. Accurate estimation of vertical mixing can only be made using detailed high resolution observations and/or high-resolution numerical modeling. Here, we provide some very preliminary generic estimates of possible mixing scales based on typical oceanic conditions.

Direct measurements of vertical turbulence mixing and diffusion in the ocean have yielded vertical mixing coefficients over a wide range of values [cf. *Gargett*, 1989; *Gargett and Marra*, 2002]. In particular, *Gregg* [1991] indicated that they can vary from $10^{-5} \text{ m}^2\text{s}^{-1}$ to $10^{-3} \text{ m}^2\text{s}^{-1}$, where the smaller values correspond to "typical" open-ocean conditions, while higher values are related to specific regions, such as the Scotia Sea where the Antarctic Circumpolar Current flows between Antarctica and South America [*Garbato et al.*, 2004]. It is unlikely that Milne Inlet is such a "specific place"; thus, we expect mixing coefficients to be in the range $10^{-5} \text{ m}^2\text{s}^{-1}$ to $10^{-4} \text{ m}^2\text{s}^{-1}$. In summer, during open-water conditions, mixing is determined by the turbulence flux from wind forcing, while in winter the mixing is probably related to the freezing of salty water that releases salt into the water column and creates vertical convection.

Table 12. The vertical plume scale (in m) for different mixing coefficients and time periods.

Mixing coefficient (m^2s^{-1})	Plume thickness (m) for specified durations		
	45 days	90 days	365 days
10^{-5}	6.2	8.8	17.8
$3 \cdot 10^{-5}$	10.8	15.2	30.8
10^{-4}	19.6	17.8	56.3

8. Estimation of water property change in Milne Inlet due to summer operations

Ballast water discharged into Milne Inlet will disperse due to horizontal advection and vertical mixing. According to the previous section, we estimate a typical vertical extension of the initial plume of about 20-50 m (see Table 12). The horizontal extension of the plume is controlled by wind-induced and estuarine circulation (during the open-water season) and by tidal excursions (year-around). The main contribution to the horizontal spreading of the plume is likely to be from wind-induced currents. These currents, along with the estuarine circulation, create a near-uniform

summer circulation in the inlet. According to Table 11, the horizontal dispersion by summer advection is several tens of kilometers, significantly exceeding the length of the southern part of the inlet (Assumption Harbour, see Figure 5). This tidal excursion will persist throughout the entire year and will create back-and-forth movements in the inlet of much smaller scale (up to 350 m, see Table 10). The Assumption Harbour area is about 36.2 km² (Table 9); from this, we can estimate the yearly volume of the plume using the vertical scale data from Table 12. The final (year-around) concentration c_f of the ballast water in the plume can be estimated from a simple formula

$$c_f = \frac{V_{ballast}}{Ad} \quad (16)$$

where V_b is the total water discharge, A is the final horizontal area of the plume and d is the final plume thickness. The final change in a given water property $\Delta\theta$ (e.g., salinity, temperature or density) inside the plume can be estimated as

$$\Delta\theta_f = c_f (\theta_{ballast} - \theta_0), \quad (17)$$

where the indices “ f “ and “0” denote the final value and the initial values.

The calculated changes in salinity, temperature and water density due to one-year of operations are presented in Table 13. **It is evident that the estimated changes in water properties are only small fractions of the natural water changes in this area.** For example, the change in salinity of ~1 psu at 30 m depth induced by the ballast water discharge in August 2010 was significantly smaller than that observed between the June and September 2008 surveys. Substantial natural salinity variations are related to the sea ice melting-freezing cycle, which depends on conditions in a particular year. The expected changes in salinity due to the ballast water discharge are approximately three orders of magnitude (1/1000) smaller than those due to natural salinity changes. The same conclusion can be made about temperature and density variations in the area under study.

Table 13 Changes in water properties during one year operation. The discharge volume is 645,000 m³, the initial salinity difference is 2.0 psu, the initial temperature difference is 6°C, and the initial density difference is 1 kg m⁻³

Plume thickness (m)	Plume area (km ²)	Final concentration	Change in salinity (psu)	Change in temperature (°C)	Change in density (kg m ⁻³)
20	36.2	0.0009	0.0018	0.0054	0.0009
50	36.2	0.00035	0.0007	0.0022	0.00035

9. Conclusions

The empirical and analytical results presented in this report indicate that ballast water discharged from the port and starboard sides of vessels docked in Milne Inlet in summer time will merge within minutes into a single gravity current which will flow downslope at speeds of 0.06 to 0.24 ms⁻¹ (~0.1 to 0.5 knots). The offshore extent of the ballast water gravity current is determined primarily by the reduction in bottom slope, which for the vicinity of the docked vessel, changes from roughly 10° near the vessel to less than 2° beginning around 700 to 900 m seaward of the vessel. Water depths over this distance increase from roughly 30 m under the ship to 100 m at 900 m offshore. It will take the head of the gravity current of about 1.5-4 hrs to travel the 900 m to the base of the slope. Tidal currents are weak in Milne Inlet, even during times of maximum tidal flow, so that tidal currents will have little time to deflect gravity currents from their downslope course. In all instances, offshore pooling of the ballast water is therefore likely to occur directly offshore, less than one kilometer from the vessel.

Over the summer discharge period, the gravity currents will diffuse laterally and vertically due to the effects of background turbulence and current associated with tidal, wind-driven and estuarine circulation. We estimated tidal water excursion using observations at a nearby tide gauge and a simple barotropic one-dimensional model. Our findings indicate that horizontal tidal excursion has a range from 140 m to 330 m. Using parameters typical for the inlet circulation conditions, we estimated a range of wind-induced and estuarine currents in the inlet. It is shown that the horizontal extension of the initial plume can likely occupy the full southern narrow part of Milne

Inlet (Assumption Harbour). Vertical mixing during the summer operational season and winter ice-covered conditions will extend the thickness of the initial plume up to 20-50 m. The lateral and vertical expansion of the plume leads to a decrease in the concentration of the ballast water in the plume, which at the end of the year will be as small as 10^{-3} (~0.1%). The decrease in concentration, in turn, will adjust the physical parameters inside the plume to natural values. **The final (year-round) change in water properties will contribute only a small fraction (about 0.1%) of typical natural changes of water properties occurring in the inlet on annual basis.**

10. References

Britter, R.E. and Linden, P.F. (1980), The motion of a front of a gravity current travelling down an incline. *J. Fluid Mechanics*, 99, 531-543.

Church, I., Hughes Clarke J.E., and Haigh, S. (2007), Use a nested finite-element hydrodynamic model to predict phase and amplitude modification of tide within narrow fjords, U.S. Hydro, May 2007, 1-16.

Fissel, D.B. (1982), Tidal currents and inertial oscillations in northwestern Baffin Bay. *Arctic*, 35 (1), 201-210.

Fissel, D.B., Lemon, D.D., and Birch, J.R. (1982), Major features of the summer near-surface circulation of western Baffin Bay, 1978 and 1979. *Arctic*, 35 (1), 180-200.

Gargett, A.E. (1989), Ocean Turbulence. *Annual Review of Fluid Mechanics*, vol. 21, 419-451; doi: 10.1146/annurev.fl.21.010189.002223.

Gargett, A.E, and Marra, J. (2002), Effects of upper ocean physical processes - turbulence, advection, and air-sea interaction - on oceanic primary production. In: *The Sea, Vol.12* (Edited by A. R. Robinson, J. J. McCarthy, and B. J. Rothschild), John Wiley and Sons, NY, 19-49.

Gill, A.E. (1982), *Atmosphere-Ocean Dynamics*. Academic Press, 662 p.

Garabato A.C.N., Polzin, K.L., King, B.A., Heywood, K.J., and Visbeck, M. (2004), Widespread intense turbulent mixing in the Southern Ocean. *Science*, 303 (5655), 210–213.

Gregg, M.C. (1991), The study of mixing in the ocean: a brief history. *Oceanography*, 4 (1), 39–45.

Kulikov, E.A., Rabinovich, A.B., and Carmack, E.C. (2004), Barotropic and baroclinic tidal currents on the Mackenzie shelf break in the southeastern Beaufort Sea *J. Geophys. Res.*, 109, C05020, 3069, 1-18; doi:10.1029/2003JC001986.

McLaughlin, F.A., Carmack, E.C., Ingram, R.G., Williams, W.J., and Michel, C. (2006), Oceanography of the Northwest Passage. In: *The Sea. Vol. 14, The Global Coastal Ocean* (Edited by A.R. Robinson and K.H. Brink), Harvard University Press, Cambridge, MA, 1213-1244.

Munk, W.H., and Phillips, N. (1968), Coherence and band structure of inertial motion in the sea, *Rev. Geophys.*, 6, 447-472.

Stewart, R.H. (2009), *Introduction to Physical Oceanography*, http://oceanworld.tamu.edu/ocng_textbook/contents.html.

Tang, C.C.L, Ross C.K., Yao, T., Petrie, B., DeTracey, B.M., and Dunlup, E. (2004), The circulation, water masses and sea-ice of Baffin Bay, *Progress in Oceanography*, 63, 183-228.